Aircraft Observations for Improved Physical Parameterization for Seasonal Prediction

Qing Wang
Meteorology Department, Naval Postgraduate School
Monterey, CA 93943
Phone: (831) 656-7716, Fax: (831) 656-3061 email: qwang@nps.edu

Award # N0001413WX20180

Anthony Bucholtz
Naval Research Laboratory, 7 Grace Hopper Ave, Monterey, CA
phone: (831) 656-5024 fax: (831) 656-4769 email: anthony.bucholtz@nrlmry.navy.mil

Award # N0001413WX20179

LONG-TERM GOAL

The long-term goal of this project is to improve the representation of fractional low-level clouds in the medium-range forecast models.

OBJECTIVES

The objectives of the NPS project is to understand the physical processes involved in boundary layers covered by fractional cloudiness and to make extensive measurements to address critical issues in cloud and turbulence parameterizations for improvements of extended forecasts.

The objectives of the NRL project are to obtain measurements of the solar and IR irradiance throughout the cloudy boundary layer in order to characterize the solar and IR radiative energy environment. In particular, to obtain vertical profiles of the solar and IR irradiance throughout the boundary layer to quantify the role of the solar and IR heating/cooling rate profiles on marine stratus.

APPROACH

The general approach of NPS research in this project is to understand the physical processes in stratocumulus-topped boundary layers through extensive data analyses of measurements from boundary layers with various macrophysics properties of stratocumulus clouds. To achieve the research goal on improving physical parameterizations used in the forecast models, collaborations with other researchers in this DRI group is necessary. We made extensive field measurements in August/September of 2012 in cloud and boundary layer conditions that were not sampled by previous stratocumulus cloud related field programs. Data from previous field programs are also analyzed to compliment the new data from our measurements in 2012. The field campaign using the CIRPAS Twin Otter, which occurred in August/September 2012, will be referred to as Unified Physical Parameterization for Extended Forecast 2012 field project (UPPEF2012).

Report Documentation Page

Form Approved
OMB No. 0704-0188

1. REPORT DATE	2. REPORT TYPE	3. DATES COVERED
30 SEP 2013		**00-00-2013 to 00-00-2013**

4. TITLE AND SUBTITLE	5a. CONTRACT NUMBER
Aircraft Observations for Improved Physical Parameterization for Seasonal Prediction	5b. GRANT NUMBER
	5c. PROGRAM ELEMENT NUMBER
6. AUTHOR(S)	5d. PROJECT NUMBER
	5e. TASK NUMBER
	5f. WORK UNIT NUMBER
7. PERFORMING ORGANIZATION NAME(S) AND ADDRESS(ES) **Naval Postgraduate School,Department of Meteorology,Monterey,CA,93943**	8. PERFORMING ORGANIZATION REPORT NUMBER
9. SPONSORING/MONITORING AGENCY NAME(S) AND ADDRESS(ES)	10. SPONSOR/MONITOR'S ACRONYM(S)
	11. SPONSOR/MONITOR'S REPORT NUMBER(S)

12. DISTRIBUTION/AVAILABILITY STATEMENT
Approved for public release; distribution unlimited

13. SUPPLEMENTARY NOTES

14. ABSTRACT

15. SUBJECT TERMS

16. SECURITY CLASSIFICATION OF:			17. LIMITATION OF ABSTRACT	18. NUMBER OF PAGES	19a. NAME OF RESPONSIBLE PERSON
a. REPORT **unclassified**	b. ABSTRACT **unclassified**	c. THIS PAGE **unclassified**	**Same as Report (SAR)**	**8**	

For the NRL project, identical pairs of customized pyranometers and pyrgeometers were mounted on the top and bottom of the CIRPAS Twin Otter aircraft to directly measure the down- and up-welling solar and infrared irradiance in the boundary layer. These instruments were commercially available solar and IR radiometers modified for aircraft use.

Qing Wang is responsible for the overall project. In FY13, analyses of the UPPEF measurements were aided by LCDR Pamela Tellado as part of her thesis research. NRC postdoc, Dr. Denny Alappattu, were also involved in the data analyses of UPPEF2012. Mr. Kurt Nielsen assisted in satellite data collection and basic analyses through collaboration with Dr. Jeff Hawkins' group at NRL Monterey.

WORK COMPLETED

Our work in FY13 focused on documentation and analyses of UPPEF2012 field campaign. Specific work done includes:

1. Preliminary analyses of all UPPEF2012 measurements from 12 flights for purpose of generating field campaign summary to be distributed to the UPPEF DRI community. The analyses include producing flight tracks, modular flight leg information, satellite imageries overlaid with flight tracks, and analyses and summary of synoptic conditions. All results of this work went into the UPPEF measurement summary delivered to interested DRI participants.
2. An overview analyses of all UPPEF2012 flights to identify cases for specific research issues to take into consideration cloud conditions, SST variability, and length and altitude of measurement legs suitable for in-depth analyses. The purpose of this analyses is to initiate joint observation/modeling research efforts by the UPPEF DRI group by making recommendations of 'good cases' for focused modeling efforts of the UPPEF modeling participants. Suggested cases have been presented to interested UPPEF modeling group for open discussions on choices of cases for future modeling efforts. This collaborative effort is ongoing.
3. Extensive analyses of selected cases with the focus on SST variability and cloud variability.
4. Under the NRL project, post-mission calibrations were carried out and analyzed at the CIRPAS Radiometer Calibration Lab. Pre- and post-mission calibrations were then used in the processing and quality-control of the NRL solar and IR broadband radiometer irradiance data. QC'ed datasets, with documentation, of the solar and IR irradiance measured on each flight of the CIRPAS Twin Otter aircraft during UPPEF were submitted to the NPS UPPEF data archive.

RESULTS

UPPEF measurement summary: During UPPEF2012, 12 CIRPAS Twin Otter flights were made west of Monterey Bay in a variety of cloud conditions. Several different flight patterns were also used for different cloud structure and boundary layer conditions. Figure 1a shows the flight tack of all flights in UPPEF to illustrate the geographical location of the measurements and the variety of flight patterns were used (e.g., S-pattern, U-pattern, L-pattern, or straight leg pattern). The selection of a specific flight pattern was determined by many factors including the cloud structure and the main objective of the flight mission. A few long single cross-wind legs were used in some of the flights in conditions where mesoscale cloud features were identified. However, what seems to be a straight leg may not have been flown at the same altitude mainly due to the changing cloud top height that varied from east to west. Figure 1b summarized the time of the day for all flights. The use the Controlled Towing Vehicle (CTV) are indicated on this figure, too. Figure 2 shows an example of the variable nature of the cloud layer on Sept 6, 2012. The cloud layer on this day had apparent mesoscale feature in the north-south direction. The multi-scale nature of the cloud structure is also seen in the region of the

aircraft sampling. Such variability of the cloud structure will be studied in future research using a combination of aircraft data with satellite cloud imageries.

The east-west variability of cloud and the boundary layer was the main feature frequently observed during UPPEF measurements because of the proximity of the measurement region to the coast. Figure 3 shows the composite boundary layer height obtained from all aircraft soundings from 12 UPPEF2012 Twin Otter flights. The four panels in Fig. 4 show the cloud and boundary layer variability from one flight on RF02 (4 Sept. 2012). In this example, the approximate slope for the BLH is estimated to be 2 m per kilometer. The figure shows the upward tilt in the cloud top and base with cloud thickness slightly increasing offshore and thickest near 122.9W . The q_c increases from the base of the cloud with maximum values (>0.4 gkg^{-1}) near the cloud top. Specific humidity (Fig. 4b) is high and fairly uniform with height in the boundary layer and through the cloud top, decreasing rapidly above the cloud top height. There is also greater moisture in the boundary layer offshore (9 gkg^{-1}) than near the coast (7.1 gkg^{-1}) corresponding to higher SST away from the coast. At the top of the boundary layer, there is an inversion of almost 10K in an approximately 50m thick layer. Potential temperature increases to approximately 305K above the boundary layer. The near-surface θ are about 2K colder near the coastal waters than offshore and consistent with the water temperature below. The first sounding was at takeoff from the Marina airport and experienced slightly higher θ (about 2K) than the upwelled coastal waters. The wind (Fig. 4d) is strongest offshore (8 m s^{-1}) in the boundary layer, decreases to 2 m s^{-1} above the cloud layer. Each of the variables displayed typical stratocumulus profiles (e.g., Nicholls 1984).

Turbulent surface fluxes in response to strong SST variability: For a larger scale variability of SST field, we downloaded a graphical representation of the Global 1 km SST (G1SST) field provided by NASA Jet Propulsion Laboratory (JPL) for the gap-free blended SST along the US West Coast. The image for 31 August 2012 is overlaid in Google Earth with the RF01 flight track and level legs in the cold and warm sectors of the SST front (Fig. 5). The sharp SST front is evident in the image along the red and purple legs and corresponds to the SST front revealed by the UPPEF 2012 data (Fig. 6).

Two levels of legs were flown over the SST front, LL9 and LL10 were flown just under 100m, while LL7, LL8, LL11, and LL12 were flown closest to the surface (~30m, refer to Fig. 6 for location of these legs). Time series of SST, θ, q, wind speed, wind direction, and pressure comparing the LL7 and LL12 are shown in Fig. 7a. LL7 and LL12 overlay each other at an altitude of 35m, with LL7 passing the SST front 53 minutes before LL12. Overall, the time series match fairly well for LL7 and LL12, and suggests not much temporal variability for the SST front during the flight, except the wind direction had a more northerly component in LL7. The warm sectors have warmer temperature and slightly dries air compared to the cold sectors. Meanwhile, the warm sectors appear to have slightly stronger wind speed and significantly increased turbulence as evidence in wind and water vapor perturbations.

The variation of sensible heat (SHF) and latent heat fluxes (LHF), stress, and air-sea temperature difference from LL7 are shown in Fig.7b. In all of the plots, turbulence is greater in the warm SST region (west of front) compared to the cold SST regions (east of front). Table 1 provides the calculated mean values of each variable for all relevant legs prepared into warm (top table) and cold (bottom table) regions. A quick glance at Table 1 indicates significant differences in all variables similar to those shown in Fig. 7b. The warm region has near surface (~30 m) SHF in the range of 6-13 Wm^{-2}, LHF of 90-118 Wm^{-2}, and stress between 0.30-0.37 Nm^{-2}, and negative air-SST difference (unstable stratification). In contrast, the cold water region are stably stratified with air-sea temperature difference between 0.6 and 1.8^{o}C, resulting in small but consistently negative SHF at both levels. The wind stress is very weak over the cold water region, too. Latent heat flux are small, too, but

consistently positive. Water vapor supply to the boundary layer over the cold region is definitely much weaker compared to the warm region. Wind speed was observed to be consistently weaker over the cold region compared to its warm neighbor (Table 1). The weaker speed on the cold side of a SST front is primarily due to the stable boundary layer formed over cold SST, which leads to a very shallow BL and thus a strong momentum flux convergence to reduce the wind speed (Skyllingstad et al., 2007). Some flux divergence are seen over the warm water region, the divergence is not apparent over the cold water region, likely imbedded in the sampling error in the fluxes of smaller magnitudes.

REFERENCES:

Nicholls, S., and J. D. Turton, 1984: An observational study of the structure of stratiform cloud sheets: Part II. *Quart. J. R. Met. Soc.*, **112**, 461–480.

Skyllingstad, E. D., D. Vickers, L. Mahrt, and R. Samelson, 2007: Effects of mesoscale sea-surface temperature fronts on the marine atmospheric boundary layer. *Bound. Layer Meteor.*, **123**, 219–237.

IMPACT/APPLICATIONS

Analyses of UPPEF2012 data provide the basis of case selection for ongoing UPPEF modeling efforts. The new measurements by the CIRPAS Twin Otter under this project have proved to be a valuable dataset to further our understanding of physical processes affecting fractional clouds and therefore for obtaining improved parameterization in fractional cloud condition in forecast models.

The radiometer measurements (NRL effort) are important to this study because the solar radiative heating and IR radiative cooling are two of the primary drivers of turbulent processes in marine stratus and in the evolution and persistence of these clouds.

RELATED PROJECTS

Related project is the ONR DRI on Unified Physical Parameterization for Extended Forecast.

PUBLICATIONS

Tellado, Pamela A. 2013: Physical processes in Coastal Stratocumulus clouds from aircraft measurements during UPPEF 2012, MS. Thesis, Naval Postgraduate School, September 2013.

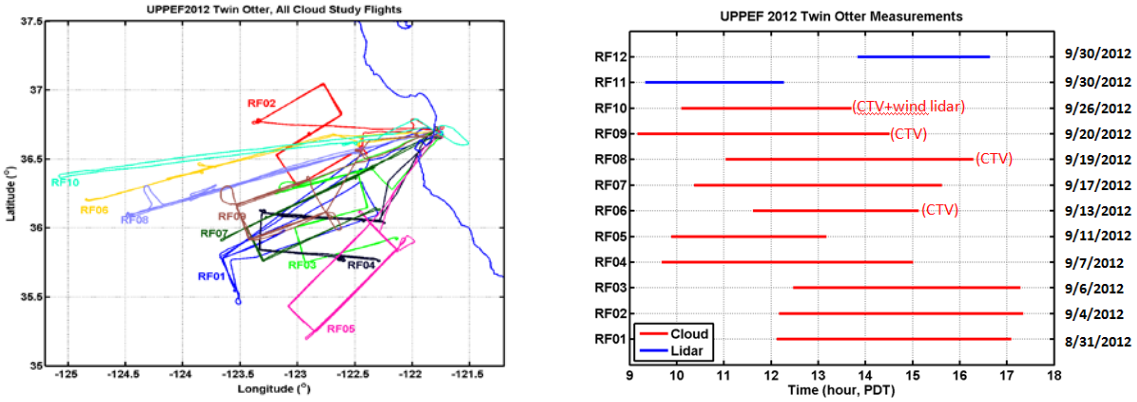

Figure 1. Summary of flight tracks and time of measurements for all UPPEF2012 Twin Otter flights.

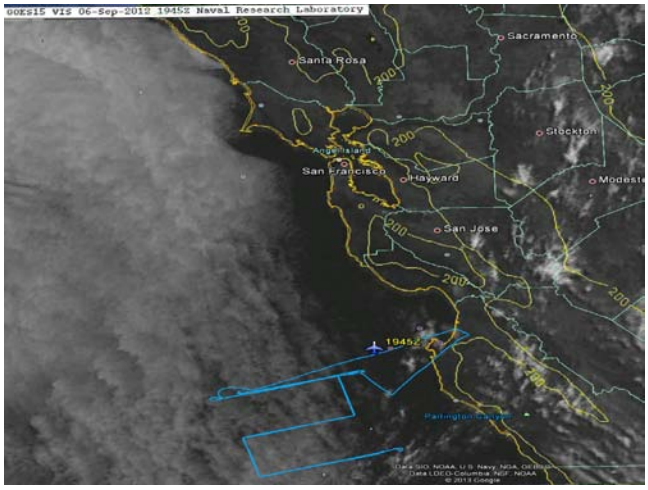

Figure 2. An example of complicated fractional cloud structure sampled on September 6, 2012. Flight track of RF03 is overlaid on the GOES satellite imagery.

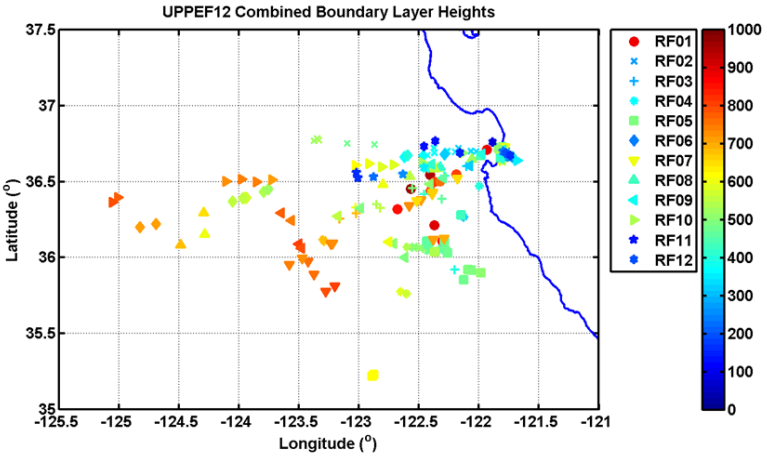

Figure 3. Spatial variability of boundary layer heights from ALL UPPEF2012 flights.

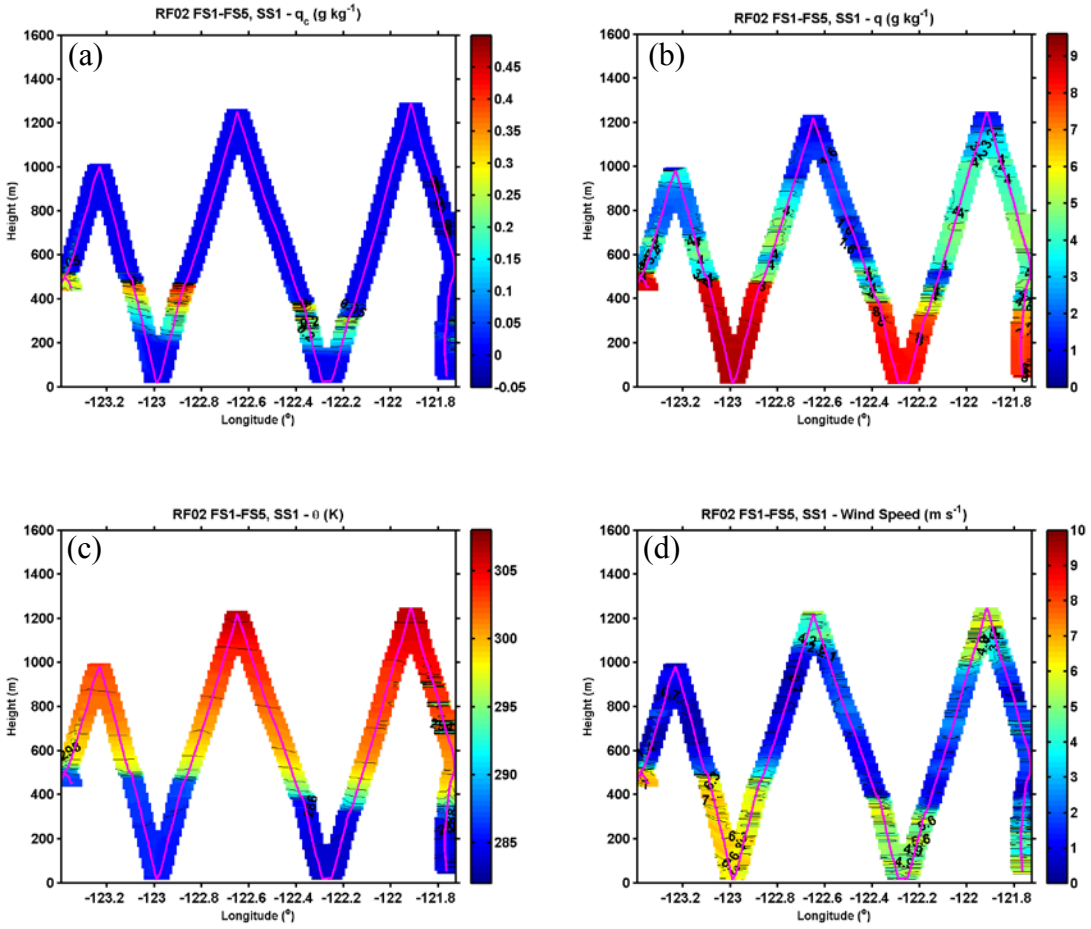

Figure 4. East-west variation of boundary layer structure from multiple soundings by the Twin Otter on 4 September, 2012. (a) Cloud liquid water; (b) water vapor specific humidity; (c) virtual temperature; and (d) horizontal wind speed.

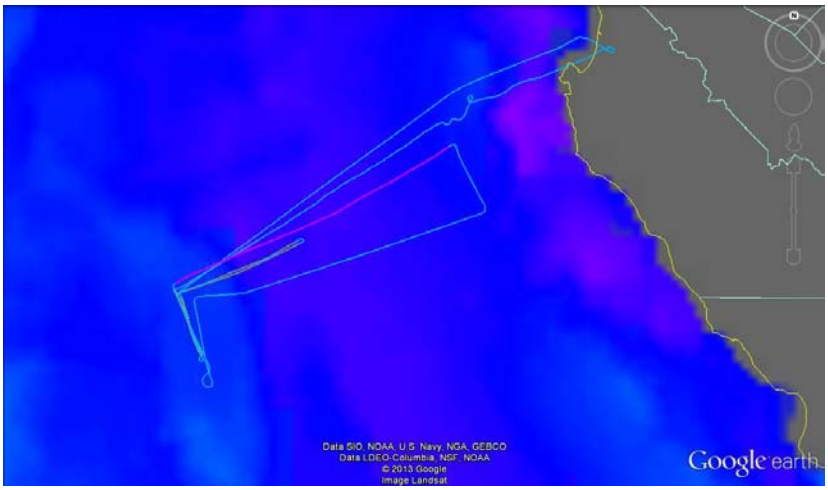

Figure 5. NASA JPL 1km Global SST (G1SST) for 31 August 2012 overlaid on Google earth with RF01 flight track (light blue line), with LL7 and LL12 (purple lines), LL8 and LL9 (orange lines), and LL10 and LL11 (red lines).

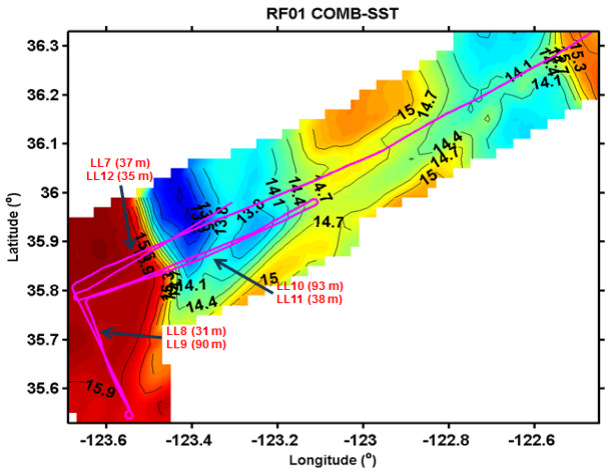

Figure 6. Contour plot for SST during RF01. Flight tracks are represented by magenta solid line. Near surface LL7, LL12, LL10 and LL11 crossed over the strong SST gradient. Near surface LL8 and LL9 are in the warm SST region, as indicated.

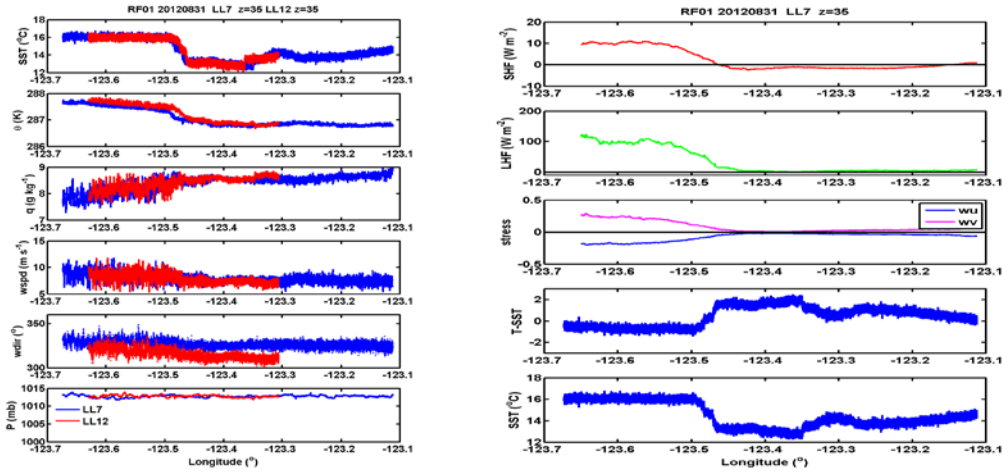

Figure 7. Variability with longitude from two near-surface legs (LL7 and LL12) on RF01 for (a) SST, θ, q, wind speed, wind direction, and pressure, and (b) Sensible heat flux (SHF), latent heat flux (LHF), wind stress, difference of air temperature and SST (T-SST), and SST.

Table 1. Comparison of mean and turbulent fluxes over warm and cold SST regions.

RF01 Mean variables	LL11 (z=38m) Warm	LL10 (z=93m) Warm	LL7 (z=35m) Warm	LL12 (z=35m) Warm	LL8 (z=31m) Warm	LL9 (z=90m) Warm
SHF (Wm^{-2})	9.0964	6.4384	10.2287	13.2936	5.8609	4.1867
LHF (Wm^{-2})	117.8148	117.1868	104.0729	89.4846	100.1591	43.9612
Stress (Nm^{-2})	0.3621	0.3592	0.2957	0.3741	0.1022	0.1061
Wind Speed (ms^{-1})	8.933	9.3587	8.9654	8.5702	9.9017	9.388
Wind Direction (°)	327.4332	320.9001	329.9618	320.5	329.6294	330.5528
θ -SST (K)	-0.4932	-1.0551	-0.6582	-0.471	-0.3841	-0.8582
SST (°C)	15.9801	15.9686	16.0799	15.9975	15.9687	15.8803

RF01 Mean variables	LL11 (z=38m) Cold	LL10 (z=93m) Cold	LL7 (z=35m) Cold	LL12 (z=35m) Cold
SHF (Wm^{-2})	-0.9813	-0.6611	-1.5665	-1.3253
LHF (Wm^{-2})	3.263	4.5991	4.7319	5.227
Stress (Nm^{-2})	0.0268	0.0319	0.024	0.0352
Wind Speed (ms^{-1})	7.4146	9.0964	7.6675	7.2658
Wind Direction (°)	320.786	317.434	325.0623	312.0479
θ -SST (K)	0.9381	0.6315	1.6552	1.8199
SST (°C)	13.7164	13.758	13.0769	12.977